International Journal of Multiphase Flow 36 (2010) 439–448

Contents lists available at ScienceDirect

International Journal of Multiphase Flow

journal homepage: www.elsevier.com/locate/ijmulflow

Review

Modeling of three-phase heavy oil–water–gas bubbly flow in upward vertical pipes

O. Cazarez [a,*], D. Montoya [a], A.G. Vital [b], A.C. Bannwart [c]

[a] Instituto Mexicano del Petróleo, Eje Central Lázaro Cárdenas No. 152, Col. San Bartolo Atepehuacan, C.P. 07730, México D.F., Mexico
[b] Centro Nacional de Investigación y Desarrollo Tecnológico, Depto. de Mecánica, Interior Internado Palmira s/n, Col. Palmira, Cuernavaca, Morelos, Mexico
[c] Dept. of Petroleum Engineering, Faculty of Mechanical Engineering, The State University of Campinas, 13083-970 Campinas, SP, Brazil

ARTICLE INFO

Article history:
Received 8 July 2009
Received in revised form 5 January 2010
Accepted 22 January 2010
Available online 2 February 2010

Keywords:
Three-phase flow
Bubbly gas–bubbly oil
Heavy oil
Two-fluid model

ABSTRACT

A bubbly gas–bubbly oil flow pattern may occur when water, heavy oil and gas flow simultaneously in vertical pipes in such a way that water is the continuous phase. In this work, a one-dimensional, thermal, transient two-fluid mathematical model, for such flow, is presented. The model consists of mass, momentum and energy conservation equations for every phase whose numerical solution is based on the finite difference technique in the implicit scheme. The model is able to predict pressure, temperature, volumetric fraction and velocity profiles. For accurate modeling of multiphase flows, the key issue is to specify the adequate closure relationships, thus drag and virtual mass forces for the gas and oil phases were taken into account and special attention was paid on the gas–oil drag force. When this force was included into the model it was found that: (1) such force had the same order of magnitude than the oil drag force and both forces were smaller than the gas drag force, (2) the pressure, gas and oil velocities and gas and oil volume fraction profiles were affected, (3) the numerical stability was increased. The model predictions are in agreement with experimental data reported in literature.

Contents

1. Introduction

Heavy oil–water–gas three-phase flow often occurs in the petroleum industry, for example, in onshore and offshore hydrocarbon production and transportation. Reasons for such occurrence are: (1) water is very often present in the reservoirs (i.e. connate water) and accompanies the produced oil and natural gas, which arises naturally from the reservoir and (2) water is produced due to water injection in the reservoir at a later stage of the production. Knowledge on the heavy oil–water–gas flow characteristics, such as flow patterns, pressure drop and holdups, can have significant impact on the proper design and operation of pipelines and on many flow assurance issues including hydrate formation, emulsion, wax deposition and corrosion (Zhang and Sarica, 2005). Therefore, it is necessary to develop mathematical models for the prediction of heavy oil–water–gas pipe flow behavior under different conditions.

* Corresponding author. Tel.: +52 55 91758294.
E-mail addresses: ocazarez@imp.mx, cazarez_oct@hotmail.com (O. Cazarez).

0301-9322/$ - see front matter © 2010 Elsevier Ltd. All rights reserved.
doi:10.1016/j.ijmultiphaseflow.2010.01.006

It is known that two-phase gas–liquid flows are highly complex, then, it is apparent that the addition of a third phase will increase this complexity. The major difference, between two- and three-phase flows, is that the presence of two immiscible liquids gives rise to a wider variety of flow patterns, which depend on the flow rate, thermo-physical properties of the fluids, inclination angle and diameter of the pipe. For example, Woods et al. (1998) used a Finavestan A 50 B oil, air and water and identified nine flow patterns, while Speeding et al. (2000) using the same fluids identified two new flow regimes. Oddie et al. (2003) observed six flow patterns when they used kerosene, nitrogen and water. However, Viera (2004) and Bannwart et al. (2005) observed six new flow patterns when heavy oil, gas and water flow simultaneously through a circular pipe in such a way that water is the continuous phase. On the other hand, the hydrodynamic modeling of three-phase flow is based on flow pattern definitions; more flow patterns imply more discontinuities and greater complexity in the hydrodynamic models. In the literature there is few information about three-phase flow of oil–water–gas mixtures. When the liquids and gas flow separately, three flow models are used to simulate the flow (Khor et al., 1997; Taitel et al., 1995; Ghorai et al., 2005). For example, Ghorai et al. (2005) used a steady-state two-fluid model to model a three-phase (light oil–water–gas) stratified flow in pipes. They assumed that oil is lighter that water and therefore, it flows in the middle of water and gas. However, when one or two of the phases are dispersed into another, it is necessary to do some suppositions. In general, because three-phase flow models are lacking, one treatment for three-phase flow is to combine oil and water into a single liquid phase and then modeling the system as a two-phase liquid–gas flow. In this treatment, the slip between the oil and water is ignored and a homogeneous mixture is assumed for the liquid phase (Shi et al., 2004; Zhang and Sarica, 2005; Bonizzi and Issa, 2003). For example, Bonizzi and Issa (2003) simulated three-phase (liquid–liquid–gas) stratified and slug flows. They used the one-dimensional transient two-fluid model in which the continuity and momentum equations for the two liquids (light oil and water) were combined together to obtain a new equation in terms of liquid mixture quantities.

Another treatment, of the three-phase flow, is to consider oil, water and gas as one liquid phase with mixture properties, this always that the bubbly flow is present. For example, regarding heavy oil–water–gas flow, Cazarez-Candia et al. (2009) proposed a homogeneous model to predict pressure, velocity and temperature of the mixture for the bubbly gas–bubbly oil flow. However, the model is no able to predict the parameter mentioned neither the volumetric fraction for each phase.

In the present investigation, a two-fluid transient, thermal, mathematical model is presented, the one which is able to predict pressure, volumetric fraction, temperature and velocity profiles for each phase when oil, water and gas flow simultaneously under the flow pattern known as bubbly gas–bubbly oil (Fig. 1). Regarding the closure relationships, special attention was paid upon the gas and oil virtual mass force, because this force conditionally stabilizes the numerical scheme (Lahey et al., 1980; Chung and Lee, 2001; Hatta et al., 1998; Linè and Leon-Becerril, 2001). Due to the absence, in literature, of expressions for the drag force transferred from the continuous phase to heavy oil drops (F_{Do}) the drag force transferred from a continuous phase to solid particles (Michele and Hempel, 2002) was used. The gas–oil drag force (F_{Dgo}), gas drag force (F_{Dg}) and mixture-wall friction shear stress (τ_w) were also included into the model (Mitra-Majumdar et al., 1997, 1998; Wang et al., 2006; Padial et al., 2000; Schallenberg et al., 2005; Michele and Hempel, 2002).

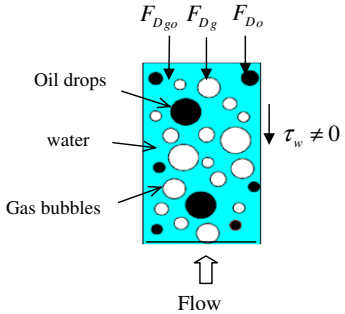

Fig. 1. Bubbly oil–bubbly gas three-phase flow [modified from Bannwart et al. (2005)].

2. Governing equations

In this work, the effects of breakup and coalescence of droplets and bubbles are neglected. The gas-wall and the oil-wall friction shear stresses (τ_{wg}, τ_{wo}) were ignored and a mixture-wall friction shear stress (τ_w) was used (Cazarez-Candia et al., 2009) at the place of a water-wall friction shear stress (Fig. 1). The drag and virtual mass forces were the only interfacial forces considered and it was supposed that the pressure in all phases are the same in a computational cell ($P = P_g = P_o = P_w$). Water and oil were treated as incompressible phases; however, the compressibility of the gas phase was taken into account. Mass transfer effects or chemical reactions have been neglected as well as the heat transfer among phases and between the flow and the wall-pipe. Then, the conservation equations of mass, momentum and energy for each phase in bubbly oil–bubbly gas three-phase flow are given by:

(i) Mass equations

$$\frac{\varepsilon_g}{\rho_g C_g^2}\left[\frac{\partial P}{\partial t}+v_g\frac{\partial P}{\partial z}\right]-\frac{\varepsilon_g}{T_g}\left[\frac{\partial T_g}{\partial t}+v_g\frac{\partial T_g}{\partial z}\right]+\left[\frac{\partial \varepsilon_g}{\partial t}+v_g\frac{\partial \varepsilon_g}{\partial z}\right]+\varepsilon_g\frac{\partial v_g}{\partial z}=0 \tag{1}$$

$$\frac{\partial(\rho_o\varepsilon_o)}{\partial t}+\frac{\partial(\rho_o\varepsilon_o v_o)}{\partial z}=0 \tag{2}$$

$$\frac{\partial(\rho_w\varepsilon_w)}{\partial t}+\frac{\partial(\rho_w\varepsilon_w v_w)}{\partial z}=0 \tag{3}$$

(ii) Momentum equations

$$\frac{\partial(\rho_g\varepsilon_g v_g)}{\partial t}+\frac{\partial(\rho_g\varepsilon_g v_g^2)}{\partial z}+\varepsilon_g\frac{\partial P}{\partial z}=-\varepsilon_g\rho_g g\sin\theta-F_{Dg}-F_{Dgo}-F_{vmg} \tag{4}$$

$$\frac{\partial(\rho_o\varepsilon_o v_o)}{\partial t}+\frac{\partial(\rho_o\varepsilon_o v_o^2)}{\partial z}+\varepsilon_o\frac{\partial P}{\partial z}=-\varepsilon_o\rho_o g\sin\theta-F_{Do}+F_{Dgo}-F_{vmo} \tag{5}$$

$$\frac{\partial(\rho_w\varepsilon_w v_w)}{\partial t}+\frac{\partial(\rho_w\varepsilon_w v_w^2)}{\partial z}+\varepsilon_w\frac{\partial P}{\partial z}=-\varepsilon_w\rho_w g\sin\theta+F_{Dg}+F_{Do}-\frac{\tau_w S_w}{A} \tag{6}$$

(iii) Energy equations

$$Cp_g\left[\frac{\partial T_g}{\partial t}+v_g\frac{\partial T_g}{\partial z}\right]+v_g\left[\frac{\partial v_g}{\partial t}+v_g\frac{\partial v_g}{\partial z}\right]-\frac{1}{\rho_g}\frac{\partial P}{\partial t}=-v_g g\cos\phi \quad (7)$$

$$\varepsilon_o\rho_o Cp_o\left[\frac{\partial T_o}{\partial t}+v_o\frac{\partial T_o}{\partial z}\right]+\varepsilon_o\rho_o v_o\left[\frac{\partial v_o}{\partial t}+v_o\frac{\partial v_o}{\partial z}\right]+\varepsilon_o v_o\frac{\partial P}{\partial z}=-\varepsilon_o\rho_o v_o g\cos\phi \quad (8)$$

$$\varepsilon_w\rho_w Cp_w\left[\frac{\partial T_w}{\partial t}+v_w\frac{\partial T_w}{\partial z}\right]+\varepsilon_w\rho_w v_w\left[\frac{\partial v_w}{\partial t}+v_w\frac{\partial v_w}{\partial z}\right]+\varepsilon_w v_w\frac{\partial P}{\partial z}=-\varepsilon_w\rho_w v_w g\cos\phi \quad (9)$$

where P is pressure, T is temperature, g is the acceleration due to gravity, ρ is density, v is velocity, ε is volumetric fraction, θ is inclination angle, $\varphi=\theta+90°$, S_w is water-wall wetted perimeter, A is the cross sectional area of the pipe, C_g is gas sound velocity, Cp is heat capacity, t and z are temporal and spatial coordinates, respectively, and F_{vm} is virtual mass force. The subscripts g, o and w represent gas, oil and water, respectively. Additionally, the following relations must be satisfied:

$$P=\rho_g RT_g \quad (10)$$

$$\varepsilon_g+\varepsilon_o+\varepsilon_w=1 \quad (11)$$

where R is the gas constant. In order to solve the system of Eqs. (1)–(11), it is indispensable to formulate appropriate closure relationships that permit modeling the interaction between phases. The closure relationships appearing in Eqs. (4)–(6) are described in Appendix A. The complete description for obtaining Eqs. (4)–(6) is presented in Appendix B.

3. Characteristics analysis

A two-fluid model for a two-phase bubbly flow is conditionally hyperbolic and therefore can be well-posed as an initial-value problem (Drew et al., 1979; No and Kasimi, 1985; Pauchon and Banerjee, 1986; Ruggles and Lahey, 1988; Espinosa-Paredes and Soria, 1998; Park et al., 1998). Then, the task here is to investigate the nature of the proposed model, and to establish whether the system is conditionally well-posed. In what follows, a study of the characteristics for the proposed set of equations is carried out.

In this work, only for the purpose of the characteristics analysis, the equations for the two liquids (oil and water) were combined to obtain the equations in terms of liquid mixture quantities. The modified system of equations is given by Eqs. (1), (12), (4), (13), (7) and (14):

$$\frac{\partial(\rho_m\varepsilon_m)}{\partial t}+\frac{\partial(\rho_m\varepsilon_m v_m)}{\partial z}=0 \quad (12)$$

$$\varepsilon_m\rho_m\frac{\partial v_m}{\partial t}+\varepsilon_m\rho_m v_m\frac{\partial v_m}{\partial z}+\varepsilon_m\frac{\partial P}{\partial z}=-\varepsilon_m\rho_m g\sin\theta+F_{Dgo}+F_{Dg}-\frac{\tau_w S_w}{A}-F_{vmo} \quad (13)$$

$$Cp_m\left[\frac{\partial T_m}{\partial t}+v_m\frac{\partial T_m}{\partial z}\right]+v_m\left[\frac{\partial v_m}{\partial t}+v_m\frac{\partial v_m}{\partial z}\right]+\frac{v_m}{\rho_m}\frac{\partial P}{\partial z}=-v_m g\cos\phi \quad (14)$$

where $\varepsilon_m=\varepsilon_w+\varepsilon_o$, $\rho_m=\frac{\rho_w\varepsilon_w+\rho_o\varepsilon_o}{\varepsilon_m}$, $v_m=v_o=v_w$, $Cp_m=\frac{\rho_w Cp_w\varepsilon_w+\rho_o Cp_o\varepsilon_o}{\rho_m\varepsilon_m}$ and $T_m=T_w=T_o$.

The modified system of equations is a system of first order partial differential equations that can be written in a compact form as:

$$\mathbf{A}\frac{\partial\mathbf{u}}{\partial t}+\mathbf{B}\frac{\partial\mathbf{u}}{\partial z}=\mathbf{C} \quad (15)$$

where $\mathbf{A}$ and $\mathbf{B}$ are coefficient matrices, $\mathbf{C}$ is a vector containing all algebraic terms and $\mathbf{u}$ is the solution vector given by:

$$\mathbf{u}=(P,\varepsilon_m,v_g,v_m,T_g,T_m)^T \quad (16)$$

where the superscript T is used to indicate the transpose. The mathematical character of a set of partial differential equations is provided by the solution of the following eigenvalue system (Hirsch, 1988):

$$\det[\mathbf{A}\lambda-\mathbf{B}]=0 \quad (17)$$

Making an order of magnitude analysis on terms in the determinant of Eq. (17), it was considered that $\rho_g C_g^2\gg\varepsilon_g$, then, the following characteristic roots were obtained:

$$\lambda=\frac{\varphi_{02}v_g+\varphi_{01}v_m\pm(v_g-v_m)\sqrt{-\varphi_{01}\varphi_{02}}}{\varphi_{01}+\varphi_{02}} \quad (18)$$

where C_g is the speed of sound into the gas phase.

In a dimensionless way λ can be written as:

$$\lambda^*=\frac{\lambda-v_m}{v_g-v_m} \quad (19)$$

In Eq. (18) φ_{01} and φ_{02} are given by:

$$\varphi_{01}=(1-\varepsilon_m)[\varepsilon_g\rho_w C_{vmg}-\rho_m] \quad (20)$$

$$\varphi_{02}=(\rho_w C_{vmg}-\rho_g\varepsilon_m) \quad (21)$$

From a mathematical point of view a system with real characteristics represents a well-posed initial-value problem and from a stability point of view the model is stable between the ranges of real characteristics. From Eq. (18), the only one condition for getting real characteristic values is when:

$$\varepsilon_g\rho_w^2 C_{vmg}^2\left(\varepsilon_g-\frac{\rho_m}{\rho_w C_{vmg}}\right)\left(1-\frac{\varepsilon_m\rho_g}{\rho_w C_{vmg}}\right)<0 \quad (22)$$

Eq. (19) and the data given in Table 1 were used to calculate λ^* (Fig. 2). It is interesting to note that the well-posed region decreases as the gas–oil volumetric fraction ratio decreases. From a physical point of view, this probably occurs because when the oil volumetric fraction increases, the coalescence phenomenon in the oil droplets begins, taking place a flow pattern transition and consequently another flow patterns may appear.

On the other hand, it is well-known that the virtual mass force conditionally stabilizes the numerical scheme, for such force a virtual coefficient is required. Then, the gas virtual coefficient, C_{vmg}, (see Appendix A) was calculated and its effect on the dimensionless characteristics was analyzed (Fig. 3). In this case gas, oil and water superficial velocities (v_{sg}, v_{so}, v_{sw}) with values of 0.05, 0.07 and 0.5 m/s were used.

Fig. 3 shows that the Eq. (22) is satisfied when: (1) the eigenvalues are always real in the interval $0<\varepsilon_g<0.176$ for different flow conditions and (2) the dimensionless characteristics of the system also vary for different values of C_{vmg}. Interestingly, a notable diminution in the well-posed region was observed when the

Table 1
Model stability region for different flow conditions.

Curve	v_{sg} (m/s)	v_{so} (m/s)	v_{sw} (m/s)	ε_g	ε_o	$\varepsilon_g/\varepsilon_o$
□	0.042	0.02	0.5	0.17681096	0.0356	4.9666
☆	0.06	0.02	0.3	0.17657821	0.0526	3.3578
△	0.048	0.04	0.5	0.17652814	0.0681	2.5921
○	0.041	0.04	0.3	0.17622005	0.1051	1.6781
◇	0.05	0.07	0.5	0.17613529	0.1129	1.5601

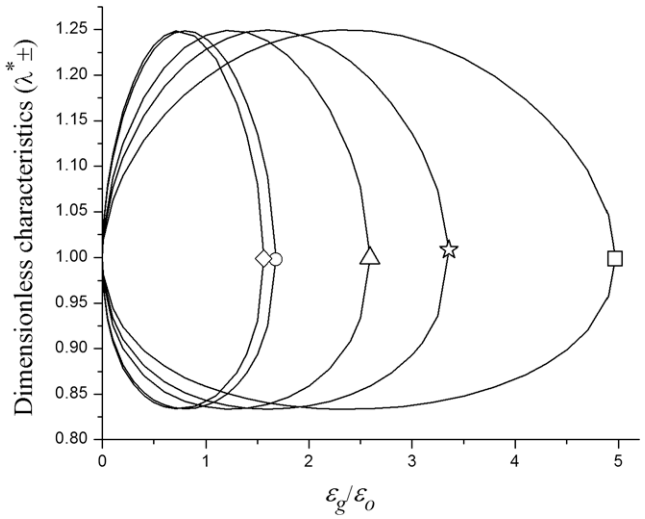

Fig. 2. Effect of oil volumetric fraction on the well-posed region.

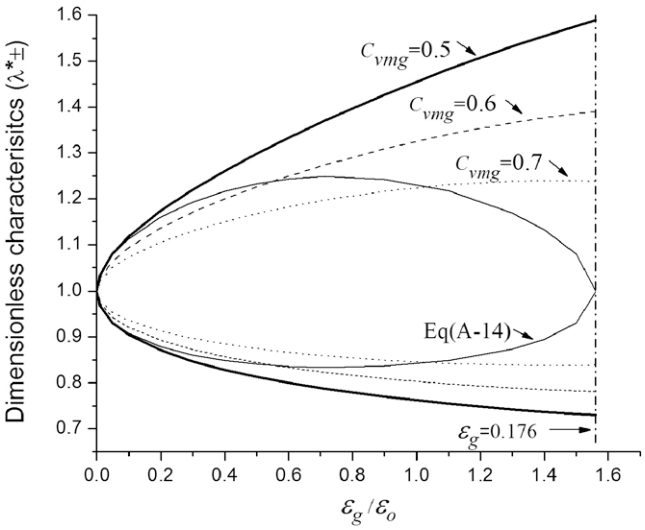

Fig. 3. Dimensionless characteristics for different values of C_{vmg}.

values of C_{vmg} are increased. In this work, the pressure, velocity, void fraction and temperature profiles were obtained using a C_{vmg} calculated from the relations proposed by Ransam et al. (1981), (Eq. (A-11) from Appendix A), whereas a value of 0.5 was used for the oil virtual mass coefficient (C_{vmo}).

4. Numerical solution

There are several numerical methods to solve partial differential equations, such as finite difference methods, finite element methods and finite volume methods. The finite difference technique is far more widely used than any other technique. This technique is implemented by replacing all derivatives by difference quotients. When the geometry is not complicated like the case of pipes, the finite difference method is easier and faster than other methods. Discretization of Eqs. (1)–(9) was obtained applying a first order downstream implicit scheme for spatial derivatives and a first order upstream implicit scheme for time derivatives. The concept of donor cell is used for parameter lumping purposes. It states that the fluid exit conditions are the same as the fluid conditions in the node itself. Stability of numerical solutions is improved using this concept. The Eqs. (1)–(9), in discretized form can be written in matrix form as:

$$\mathbf{D}_j(\mathbf{v}_j^o)\mathbf{v}_j^{t+\Delta t} = \mathbf{E}_j\left(\mathbf{v}_j^o, \mathbf{v}_j^t, \mathbf{v}_{j-1}^{t+\Delta t}\right) \tag{23}$$

where, the superscripts t and $t+\Delta t$ indicate that the dependent variables are calculated at the old and new times, respectively, and j is the cell number, where the variable is calculated. In Eq. (23), the variables with subscript $j-1$ and superscript t are known since these are the inlet variables and the initial condition, respectively. Also in these equations, the superscript o represents the dummy variables for the iterative method, **D** is the coefficient matrix, **E** is the independent vector and **v** is a column vector of dependent variables given by:

$$\mathbf{v} = \left(P, \varepsilon_o, \varepsilon_w, v_g, v_o, v_w, T_g, T_o, T_w\right)^T \tag{24}$$

where the superscript T is used to indicate the transpose.

The numerical solution of Eq. (23) was obtained using the LINPACK (Dongarra et al., 1990) package of numerical routines for solving simultaneous linear equations. The algorithm used in this study is based on the factorization of a matrix using a version of the Gaussian elimination with partial pivoting. The methodology used to obtain the numerical solution of Eq. (23), is similar to that presented in the work of Cazarez-Candia and Vazquez-Cruz (2005).

5. Results and discussion

The model is able to predict velocity, temperature, volumetric fraction and pressure profiles. The model was validated using the experimental data given by Bannwart et al. (2005), whose experiments were carried out using a crude dead heavy oil of 971 kg/m^3 with a viscosity of 5040 mPa s and a 2.84 cm i.d. and 2.5 m long vertical glass tubing. The experiments took place at ambient temperature and near atmospheric pressure. Bannwart et al. (2005) presented five different flow conditions at which the bubbly gas–bubbly oil can appear. For all these conditions the present model was tested. In Fig. 4, the predicted and experimental pressure gradients are compared. The predictions are in agreement with the experimental data, in fact the maximum error (6.52%) is reached when gas, oil and water superficial velocities (v_{sg}, v_{so}, v_{sw}) are 0.06, 0.02 and 0.3 m/s, respectively. A complete error description for different flow conditions is given in Table 2.

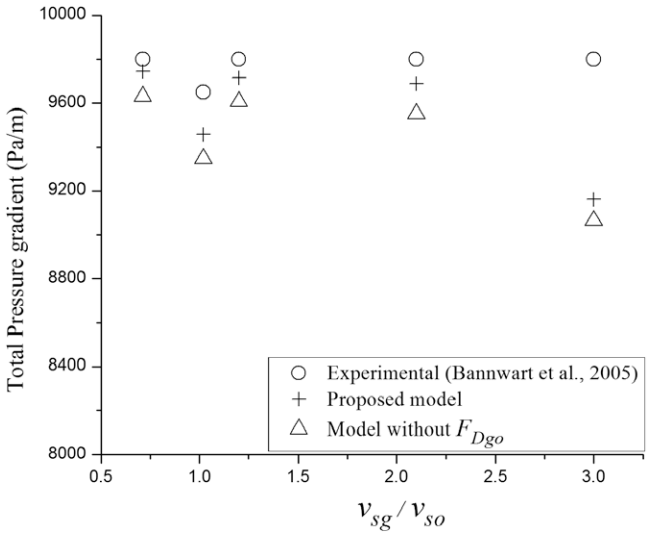

Fig. 4. Three-phase pressure gradient as a function of the gas–oil ratio.

Table 2
Error of the pressure drop prediction for different flow conditions.

v_{sg} (m/s)	v_{so} (m/s)	v_{sw} (m/s)	v_{sg}/v_{so}	Error (%)
0.05	0.07	0.5	0.712	0.55869
0.041	0.04	0.3	1.02	1.97919
0.048	0.04	0.5	1.2	0.86175
0.042	0.02	0.5	2.1	1.13767
0.06	0.02	0.3	3	6.52959

The effect of the gas–oil drag force on the pressure gradient is also presented in Fig. 4. It is shown that without the gas–oil drag force, the model predictions have notable deviations respect to the experimental data (3.38% average error) in comparison with those predictions, where the gas–oil drag force was included (2.21% average error). According to the work of Bannwart et al. (2005) for a gas–oil ratio of 3.0 also the bubbly gas–intermittent oil flow pattern may be present, this means that such conditions correspond to a transition zone. This is maybe the reason because the maximum deviation occurs when the gas–oil ratio takes a value of 3.0.

Fig. 5a shows the transient volumetric fraction profiles for each phase. The maximum value reached of water volumetric fraction was approximately 0.87, which is larger than the oil and gas volumetric fractions because the water is the dominant continuous phase according to the experimental data given by Bannwart et al. (2005).

Fig. 5b shows the velocity profiles. As it was expected the gas velocity is the largest one because its density is the smallest one. The water velocity is the smallest one, because its density is larger than the oil density ($\rho_w = 996$ kg/m^3, $\rho_o = 971$ kg/m^3) and there are two dispersed phases. This was not observed by Hatta et al. (1998) for a solid–gas–liquid three-phase flow due to the solid density ($\rho_s = 2540$ kg/m^3). Fig. 5c shows the transient pressure profiles.

On the other hand, the gas temperature profile (Fig. 5d) presented a maximum deviation of 2 K from the initial condition (298.2 K) for a short simulation time. However, when the time increases, a constant value of 298.2 K is reached. This was an expected result because it was considered adiabatic flow.

In order to improve the modeling of bubbly three-phase flow, the gas–oil drag force has to be considered, besides the well-known gas and oil drag forces. In the present work to include the gas–oil drag force into the model, a new expression is proposed, which was obtained modifying the expression given by Michele and Hempel (2002) (see Appendix A). The model increased its numerical stability when this force was taken into account.

Fig. 6 shows the comparison among different drag forces. It was found that the gas–oil drag force (F_{Dgo}) has the same order of magnitude that the oil drag force (F_{Do}) and they are smaller than the gas drag force (F_{Dg}) when the gas, oil and water superficial velocities take values of 0.06, 0.02 and 0.3, respectively. However, when gas, oil and water superficial velocities were modified (0.05, 0.07 and 0.5) a notable change was observed, since oil and gas–oil drag forces increased approximately twice as much, meanwhile the gas drag force decreased. Although changes are evident when the superficial velocities were modified, the gas, oil and gas–oil drag forces kept the same qualitative behavior at different flow conditions, where the three-phase bubbly flow appears.

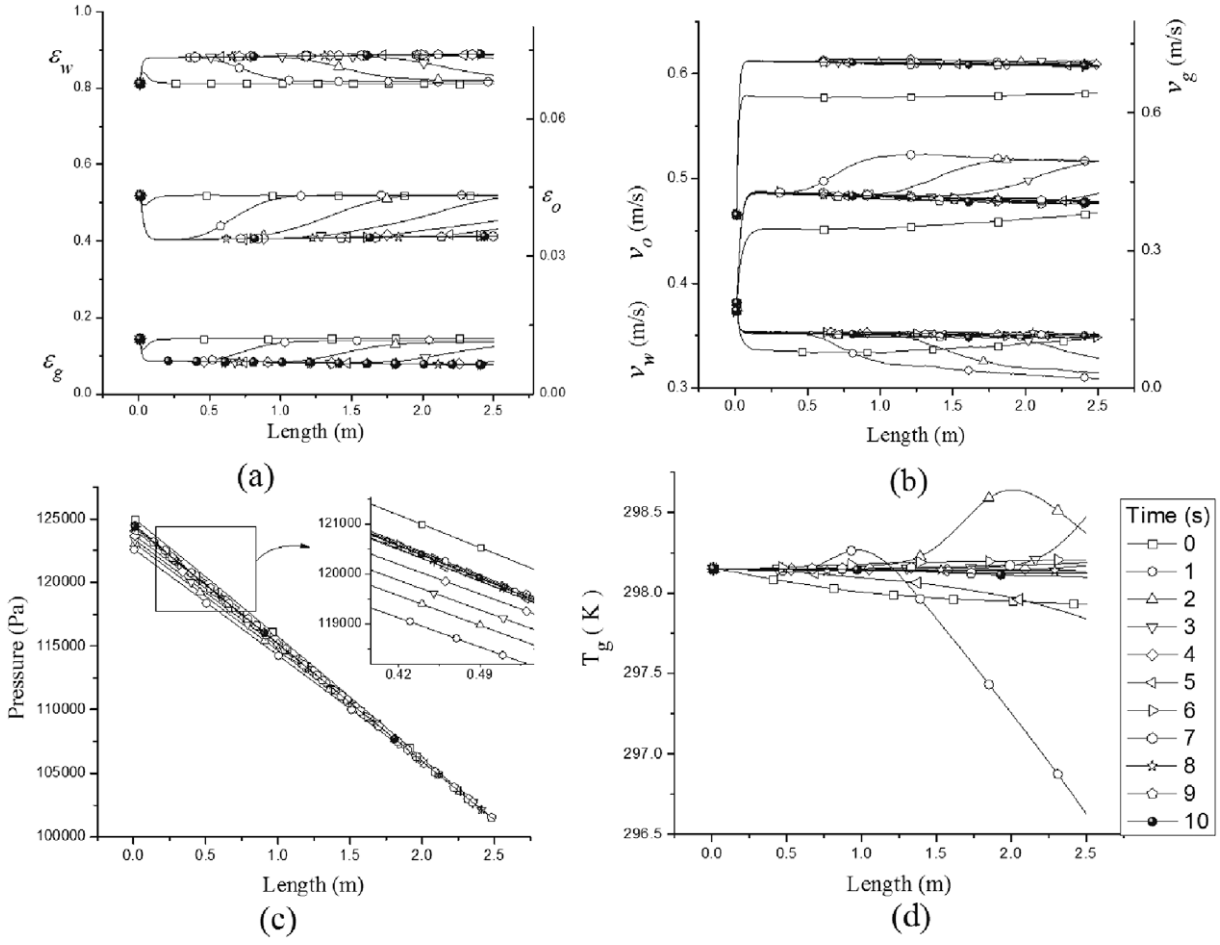

Fig. 5. Transient behavior of: (a) volumetric fractions, (b) velocities, (c) pressure and (d) temperature; for $v_{sg} = 0.06$ m/s, $v_{so} = 0.02$ m/s and $v_{sw} = 0.3$ m/s.

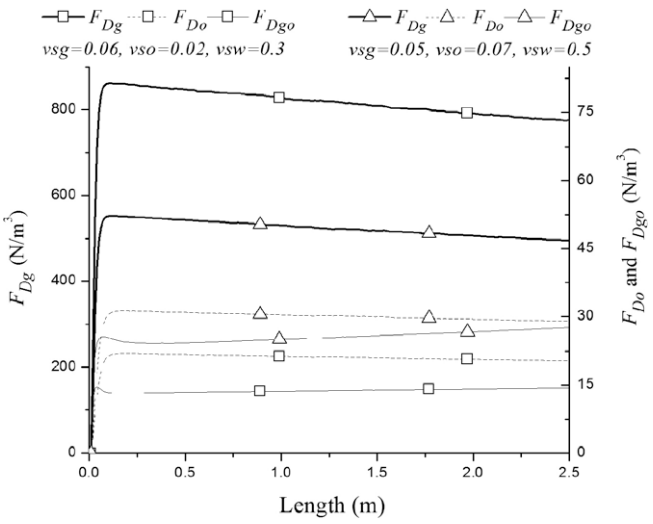

Fig. 6. Comparison among drag forces.

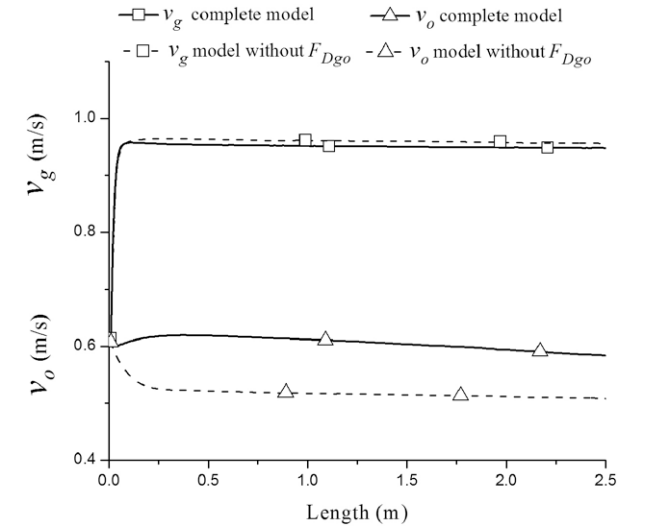

Fig. 7. Effect of the F_{Dgo} on the gas and oil velocity profiles for v_{sg} = 0.07 m/s, v_{so} = 0.05 m/s and v_{sw} = 0.5 m/s.

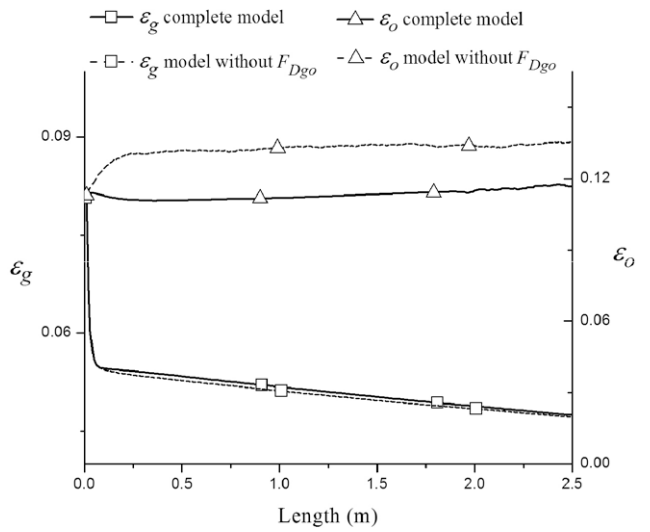

Fig. 8. Effect of the F_{Dgo} on the oil and gas volume fraction profiles for v_{sg} = 0.07 m/s, v_{so} = 0.05 m/s and v_{sw} = 0.5 m/s.

Fig. 7 shows the gas and oil steady-state velocity profiles with and without the gas–oil drag force. It can be seen that the gas phase is faster than the oil phase for both cases. This was also observed by Mitra-Majumdar et al. (1997) for a solid–gas–liquid three-phase flow. This was expected because of the large difference of densities between the phases. The inclusion of the gas–oil drag force into the model causes that the gas velocity decreases. The reason for this observation is that the presence of the oil droplets has a large hindrance to the motion of the gas bubbles. However, due to the drag of the gas phase on the oil phase, oil velocity increases when the gas–oil drag force is included into the model, this causes that the oil volume fraction decreases (see Fig. 8) and the gas volume fraction tends lightly to increase. The same qualitative behavior of gas and oil volume fraction was observed under different flow conditions, where the three-phase bubbly flow appears. The sharp variations of the oil and gas volume fractions at the inlet region are perhaps due to the arbitrary choice of volume fraction at the inlet. This arbitrariness is due to the fact that Bannwart et al. (2005) only measured superficial velocities of the phases.

6. Conclusions

A two-fluid model for three-phase bubbly gas–bubbly oil flow in vertical pipes has been presented. As is known, the key issue for the accurate modeling of multiphase flow is to specify the adequate closure relationships. For this reason, the gas–oil drag force was included in the proposed model. When such force was included, it was observed that: (1) the numerical stability was increased, (2) the gas–oil drag force had the same order of magnitude than the oil drag force and they were smaller than the gas drag force and (3) the pressure, gas and oil velocities and gas and oil volume fraction profiles were affected.

If the gas–oil drag force is not taken into account the oil velocity is smaller and the gas velocity is larger, whereas the oil volume fraction is larger and the gas volume fraction is smaller. The gas–oil drag force had not been used in previous works for modeling heavy oil–gas–water in pipes. According to the results obtained in this work it can be concluded that the use of this force enhances the capabilities of the mathematical model to predict pressure drop, volume fraction and temperature profiles of a three-phase oil–gas bubbly flow.

Regarding the pressure drop predictions, it was found that the values calculated with the model are in agreement with the experimental data reported in the literature. The maximum error value was lower than 7%.

It is expected that this model will be of benefit for further studies of heavy oil–gas–water transient multiphase flow.

Acknowledgements

The authors wish to thank the financial support provided by Consejo Nacional de Ciencia y Tecnología (CONACyT).

Appendix A

A.1. Drag forces

In the present study, the expression used for the drag force acting on a gas particle (F_{Dg}) under steady-state conditions is given in terms of the drag coefficient based on the relative velocity:

$$F_{Dg} = \varepsilon_g \rho_w C_{Dg} \frac{3}{8} \frac{|v_g - v_w|(v_g - v_w)}{R_{pg}} \quad \text{(A-1)}$$

According to Padial et al. (2000) the drag coefficient, C_{Dg}, is given as follows:

$$C_{Dg} = 1 + \frac{24}{\mathrm{Re}} + \left(\frac{6}{1+\sqrt{\mathrm{Re}}}\right) \tag{A-2}$$

The gas particle ratio R_{pg} is given by:

$$R_{pg} = \left(\frac{3V_{pg}}{4\pi}\right)^{1/3} \tag{A-3}$$

The drag force transferred from the water to the oil is given by:

$$F_{Do} = \varepsilon_o \rho_w C_{Do} \frac{3}{8} \frac{|v_o - v_w|(v_o - v_w)}{R_{po}} \tag{A-4}$$

where the drag coefficient, C_{Do}, is (Clift et al. (1978)):

$$C_{Do} = \begin{cases} \frac{24}{\mathrm{Re}}(1 + 0.15\mathrm{Re}^{0.687}); & (\mathrm{Re} \leqslant 1000) \\ 0.44; & (\mathrm{Re} > 1000) \end{cases} \tag{A-5}$$

The Reynolds number is given by:

$$\mathrm{Re} = \frac{2\rho_w |v_w - v_o| R_{po}}{\mu_w} \tag{A-6}$$

where μ_w is the water viscosity and R_{po} is the oil particle ratio given by:

$$R_{po} = \left(\frac{3V_{po}}{4\pi}\right)^{1/3} \tag{A-7}$$

To calculate the momentum transfer between two dispersed phases (gas and oil), the drag law modified from the work of Michele and Hempel (2002) was used:

$$F_{Dgo} = -F_{Dog} = \varepsilon_o \rho_g C_{Dgol} \frac{3}{8} \frac{(v_o - v_g)}{R_{po}} \tag{A-8}$$

This expression is implemented as an additional source term in the momentum equations of the gas and oil phases. In Eq. (A-8) $C_{Dgol} = C_{Dgo}|v_o - v_g|$ was used as a fitting parameter and was set constant to 138 m/s during all calculations carried out. This value may be not considered as a real physical settling velocity but is merely a fitting parameter.

Michele and Hempel (2002) found their expression from experimental data for a three-phase flow of solid particles (plexiglas granules, 1200 kg/m^3), water and air bubbles. In this work, a three-phase flow of crude oil (971 kg/m^3), water and air bubbles was modeled. The oil drops were considered perfectly spherical, and then they have a behavior similar to solid particles. Michele and Hempel (2002) reported a value for the fitting parameter of 118 m/s, whereas in this work it takes a value of 138 m/s. The difference between these values is attributed to the difference between the densities, and sizes of the solid particles and drops, and to the elastic behavior of the drops. However, it is clear that to have a better estimation of the drag force between oil drops and gas bubbles, it must be obtained from experimental data. This is a topic to be investigated.

A.2. Virtual mass force

The virtual mass force is the force required to accelerate the apparent mass of the surrounding phase when the relative velocity changes. According to Lahey (1992), the most common virtual mass force terms for gas phase as well as oil phase are given by:

$$F_{vm\ g} = \varepsilon_g \rho_w C_{vm\ g} \left[\frac{\partial v_g}{\partial t} - \frac{\partial v_w}{\partial t} + v_g \frac{\partial v_g}{\partial z} - v_w \frac{\partial v_w}{\partial z}\right] \tag{A-9}$$

$$F_{vm\ o} = \varepsilon_o \rho_w C_{vm\ o} \left[\frac{\partial v_o}{\partial t} - \frac{\partial v_w}{\partial t} + v_o \frac{\partial v_o}{\partial z} - v_w \frac{\partial v_w}{\partial z}\right] \tag{A-10}$$

where $C_{vm\ g}$ and $C_{vm\ o}$ denote the virtual mass coefficients of gas and oil phases, respectively, given by Ransam et al. (1981):

$$C_{vm\ g} = \begin{bmatrix} 0.5\left(\frac{1+2\varepsilon_g}{1-\varepsilon_g}\right); & (0 \leqslant \varepsilon_g < 0.5) \\ 0.5\left(\frac{3-2\varepsilon_g}{\varepsilon_g}\right); & (0.5 \leqslant \varepsilon_g < 1) \end{bmatrix} \tag{A-11}$$

$$C_{vm_o} = 0.5 \tag{A-12}$$

A.3. Frictional force between mixture and pipe wall

In the present model, the gas-wall friction and the oil-wall friction are neglected, and the friction force is represented by the mixture-wall interaction given by Cazarez-Candia et al. (2009):

$$\tau_w = \frac{1}{2} f_m \rho_m v_m^2 \frac{1}{d} \tag{A-13}$$

The friction factor needed to estimate the friction force can be calculated as:

$$f_m = C(\mathrm{Re})^n \tag{A-14}$$

The Reynolds number is given by:

$$\mathrm{Re} = \frac{\rho_w v_m d}{\mu_w} \tag{A-15}$$

where C and n are taken as 0.2146 and −0.25, respectively, and d is the pipe diameter. These values were used only as fitting parameters and were set constant during all calculations.

Appendix B

According to Lahey and Drew (1989) the conservation equations can be expressed as:

(i) Mass equations

$$\underbrace{\frac{\partial(\rho_k \varepsilon_k)}{\partial t}}_{\text{Accumulation}} + \underbrace{\nabla \cdot (\rho_k \varepsilon_k \mathbf{v}_k)}_{\text{Inertial}} = \underbrace{\Gamma_k}_{\text{Interfacial mass transfer}} \quad ; \quad k = o, g, w \tag{B-1}$$

In this work, the interfacial mass transfer among phases was neglected, since phase change (condensation or evaporation) phenomena did not occur. Oil and water can be supposed as incompressible phases since their compressibility is small. Under these conditions the one-dimensional equation for oil and water phases can be written as:

$$\frac{\partial(\rho_o \varepsilon_o)}{\partial t} + \frac{\partial(\rho_o \varepsilon_o v_o)}{\partial z} = 0 \tag{B-2}$$

$$\frac{\partial(\rho_w \varepsilon_w)}{\partial t} + \frac{\partial(\rho_w \varepsilon_w v_w)}{\partial z} = 0 \tag{B-3}$$

However, for the gas phase the density is function of the temperature and the pressure, then Eq. (B-1) can be expressed as:

$$\varepsilon_g \left[\frac{\partial \rho_g(T_g, P_g)}{\partial t} + v_g \frac{\partial \rho_g(T_g, P_g)}{\partial z}\right] + \rho_g \left[\frac{\partial \varepsilon_g}{\partial t} + v_g \frac{\partial \varepsilon_g}{\partial z}\right] + \varepsilon_g \rho_g \frac{\partial v_g}{\partial z} = 0 \tag{B-4}$$

where the temporal and spatial derivatives are given by:

$$\frac{\partial \rho_g(T_g, P_g)}{\partial t} = \frac{1}{c_g^2} \frac{\partial p_g}{\partial t} - \left[\frac{\rho_g}{T_g} + \frac{\rho_g}{Z} \frac{\partial Z}{\partial T_g}\right] \frac{\partial T_g}{\partial t} \tag{B-5}$$

$$\frac{\partial \rho_g(T_g,P_g)}{\partial z}=\frac{1}{c_g^2}\frac{\partial p_g}{\partial z}-\left[\frac{\rho_g}{T_g}+\frac{\rho_g}{Z}\frac{\partial Z}{\partial T_g}\right]\frac{\partial T_g}{\partial z} \tag{B-6}$$

Here c_g represents the speed of sound into the gas phase and Z is the gas compressibility factor.

Substituting Eqs. (B-5), (B-6) into Eq. (B-4) and considering ideal gas ($Z = 1$), the gas mass equation becomes as follows:

$$\frac{\varepsilon_g}{\rho_g C_g^2}\left[\frac{\partial P}{\partial t}+v_g\frac{\partial P}{\partial z}\right]-\frac{\varepsilon_g}{T_g}\left[\frac{\partial T_g}{\partial t}+v_g\frac{\partial T_g}{\partial z}\right]+\left[\frac{\partial \varepsilon_g}{\partial t}+v_g\frac{\partial \varepsilon_g}{\partial z}\right]+\varepsilon_g\frac{\partial v_g}{\partial z}=0 \tag{B-7}$$

(ii) Momentum equations

The general momentum equation is given by Lahey and Drew (1989):

$$\underbrace{\frac{\partial(\rho_k\varepsilon_k\mathbf{v}_k)}{\partial t}}_{\text{Accumulation}}+\underbrace{\nabla\cdot(\rho_k\varepsilon_k\mathbf{v}_k\mathbf{v}_k)}_{\text{Inertial}}=-\underbrace{\varepsilon_k\nabla\cdot(P_k)}_{\text{Pressure}}-\underbrace{\Delta P_{ki}\mathbf{S}_{ki}'''}_{\text{Interfacial pressure gradient}}-\underbrace{\Delta P_{kw}\mathbf{S}_{kw}'''}_{\text{Wall-phase pressure gradient}}$$
$$+\underbrace{\nabla\cdot[\varepsilon_k(\underline{\tau}_k+\underline{\tau}_k^{Re})]}_{\text{Viscous and Reynolds shear stresses}}+\underbrace{\varepsilon_k\rho_k\mathbf{g}}_{\text{Gravity force}}+\underbrace{\Gamma_k\mathbf{v}_{ki}^{\Gamma}}_{\text{Interfacial mass transfer}}+\underbrace{\mathbf{M}_{ki}^{nd}+\mathbf{M}_{ki}^{d}}_{\text{Interfacial forces}}+\underbrace{\mathbf{M}_{kw}^{nd}+\mathbf{M}_{kw}^{d}}_{\text{Wall-phase forces}}+\underbrace{\underline{\tau}_{ki}\cdot\mathbf{S}_{ki}'''}_{\text{Interfacial shear stress}} \tag{B-8}$$

where

$$\mathbf{M}_{ki}^{nd}=\mathbf{F}_{vmk}+\mathbf{F}_{Lk}+\mathbf{F}_{Rk},\quad k=o,g,w \tag{B-9}$$

$$\mathbf{M}_{ki}^{d}=\mathbf{F}_{Dk}+\mathbf{F}_{Dkq},\quad k=o,g,w;\ \ q=g,o,w,k\neq q \tag{B-10}$$

$$\mathbf{M}_{kw}^{d}=\frac{\underline{\tau}_{kw}}{D_{Hk}},\quad k=o,g,w \tag{B-11}$$

$$\mathbf{M}_{kw}^{nd}=\mathbf{F}_{Bk}+\mathbf{F}_{LLk},\quad k=o,g,w \tag{B-12}$$

The non-drag force on the wall, $\mathbf{M}_{kw}^{nd}$, includes Basset-type ($\mathbf{F}_{Bk}$) and lateral lift-type ($\mathbf{F}_{LLk}$) forces. The functional form of this term is not well known and thus it is normally neglected (Lahey and Drew, 1989). In this work, the lift ($\mathbf{F}_{Lk}$), radial ($\mathbf{F}_{Rk}$) forces were neglected, the last one because the oil drops and gas bubbles sizes are constant. Since the phase distribution around the pipe circumference is homogeneous $\mathbf{S}_{kw}''' = 0$. There are not interfacial pressure gradient, interfacial shear stress and interfacial mass transfer among phases. The viscous and Reynolds shear stresses are normally small and often neglected (Nikitopoulos and Michaelides, 1995; Lahey, 1992; Lahey and Drew, 1989). Since the dispersed phases are oil and gas, $(\mathbf{F}_{vmw},\mathbf{F}_{Dw},\mathbf{F}_{Dwg},\mathbf{F}_{Dwo})=0$.

Under these conditions the one-dimensional equation for each phase can be written as:

$$\frac{\partial(\rho_g\varepsilon_g v_g)}{\partial t}+\frac{\partial(\rho_g\varepsilon_g v_g^2)}{\partial z}+\varepsilon_g\frac{\partial P}{\partial z}=-\varepsilon_g\rho_g g\sin\theta-F_{Dg}-F_{Dgo}-F_{vmg} \tag{B-13}$$

$$\frac{\partial(\rho_o\varepsilon_o v_o)}{\partial t}+\frac{\partial(\rho_o\varepsilon_o v_o^2)}{\partial z}+\varepsilon_o\frac{\partial P}{\partial z}=-\varepsilon_o\rho_o g\sin\theta-F_{Do}+F_{Dgo}-F_{vmo} \tag{B-14}$$

$$\frac{\partial(\rho_w\varepsilon_w v_w)}{\partial t}+\frac{\partial(\rho_w\varepsilon_w v_w^2)}{\partial z}+\varepsilon_w\frac{\partial P}{\partial z}=-\varepsilon_w\rho_w g\sin\theta+F_{Dg}+F_{Do}-\frac{\tau_w S_w}{A} \tag{B-15}$$

where (F_{Do}) is the drag force transferred from the continuous phase to oil drops, (F_{Dgo}) is the gas–oil drag force and (F_{Dg}) is gas drag force.

(iii) Energy equations

The general energy equation is given by Lahey and Drew (1989):

$$\underbrace{\frac{\partial[\varepsilon_k\rho_k(e_k+e_k^T)]}{\partial t}}_{\text{Accumulation}}+\underbrace{\nabla\cdot[\varepsilon_k\rho_k(e_k+e_k^T)\mathbf{v}_k]}_{\text{Convection}}=\underbrace{-P_{k_i}\frac{\partial\varepsilon_k}{\partial t}}_{\text{Interfacial pressure}}+\underbrace{\frac{\partial(\varepsilon_k P_k)}{\partial t}}_{\text{Pressure}}-\underbrace{\nabla\cdot[\varepsilon_k(q_k''+q_k''^T)\mathbf{v}_k]}_{\text{Phase and turbulent heat fluxes}}$$
$$+\underbrace{\nabla\cdot[\varepsilon_k(\underline{\tau}_k+\underline{\tau}_k^{Re})\cdot\mathbf{v}_k]}_{\text{Viscous and Reynolds shear stresses}}+\underbrace{\varepsilon_k\rho_k\mathbf{g}\cdot\mathbf{v}_k}_{\text{Gravity force}}+\underbrace{\varepsilon_k q_k'''}_{\text{Heat generated}}+\underbrace{\Gamma_k e_{ki}}_{\text{Mass transfer}}+\underbrace{\mathbf{M}_{ki}^{nd}\cdot\mathbf{v}_{ki}^{nd}}_{\text{Work due to non-drag interfacial forces}}+\underbrace{q_{ki}''A_i'''}_{\text{Interfacial heat flux}}+\underbrace{\mathbf{M}_{ki}^{d}\cdot\mathbf{v}_{ki}^{d}}_{\text{Work due to drag interfacial forces}}$$
$$+\underbrace{\mathbf{v}_{ki}^{\tau}\cdot\underline{\tau}_{ki}\cdot S_{ki}'''}_{\text{Work due to interfacial shear stress}}+\underbrace{q_{kw}''A_{kw}'''}_{\text{Wall heat flux}}-\underbrace{\Gamma_k\langle\frac{\Delta\tilde{p}_k^d}{\rho_k}\rangle_i}_{\text{Drag interfacial pressure difference}} \tag{B-16}$$

According to Lahey and Drew (1989), the turbulent kinetic energy (e_k^T) is not normally a very important term in the energy equation. In any event, it is currently not well known how to model this parameter, thus it is usually neglected. The heat flux (q_k''), given by the Fourier's law, is relatively small and usually neglected. The turbulent heat flux $(q_k''^T)$ is normally neglected in the engineering

analyzes of two-phase flow. The interfacial stress tensor (τ_{ki}) is either neglected since its energy contribution is relatively small. The interfacial drag forces can contain energy fluctuations which are small, for this reason they are neglected. The interfacial pressure gradient is also neglected.

Into the model there is not mass interchange due to phase change or chemical reaction among two immiscible liquids (oil and water) and air, and then the heat exchange between the phases was ignored. Regarding to the heat transfer to/from the surroundings, it was not included into the model since there is not temperature gradient between the surroundings and the three-phase flow, this because the simulated experiments were done at ambient temperature. Then, the one-dimensional energy equation can be expressed as:

$$\frac{\partial[\varepsilon_k\rho_k e_k]}{\partial t}+\frac{\partial[\varepsilon_k\rho_k e_k v_k]}{\partial z}=\varepsilon_k\frac{\partial P_k}{\partial t}+\varepsilon_k\rho_k v_k g\cos\phi \tag{B-17}$$

Eq. (B-17) can be written as:

$$e_k\left[\frac{\partial(\varepsilon_k\rho_k)}{\partial t}+\frac{\partial(\varepsilon_k\rho_k v_k)}{\partial z}\right]+\varepsilon_k\rho_k\left[\frac{\partial e_k}{\partial t}+v_k\frac{\partial e_k}{\partial z}\right]=\varepsilon_k\frac{\partial P_k}{\partial t}+\varepsilon_k\rho_k v_k g\cos\phi \tag{B-18}$$

Substituting the Eq. (B-1) without the mass transfer term into the Eq. (B-18), the following equation is obtained:

$$\varepsilon_k\rho_k\left[\frac{\partial e_k}{\partial t}+v_k\frac{\partial e_k}{\partial z}\right]=\varepsilon_k\frac{\partial P_k}{\partial t}+\varepsilon_k\rho_k v_k g\cos\phi \tag{B-19}$$

where e_k is the specific energy defined as:

$$e_k=h_k+\frac{v_k^2}{2} \tag{B-20}$$

where its spatial and temporal derivatives are expressed by:

$$\frac{\partial e_k}{\partial t}=\frac{\partial h_k}{\partial t}+v_k\frac{\partial v_k}{\partial t} \tag{B-21}$$

$$\frac{\partial e_k}{\partial z}=\frac{\partial h_k}{\partial z}+v_k\frac{\partial v_k}{\partial z} \tag{B-22}$$

Substituting Eqs. (B-21) and (B-22) into Eq. (B-19), and dividing by $(\varepsilon_k\rho_k)$:

$$\frac{\partial h_k}{\partial t}+v_k\frac{\partial v_k}{\partial t}+v_k\frac{\partial v_k}{\partial z}+v_k^2\frac{\partial v_k}{\partial z}=\frac{1}{\rho_k}\frac{\partial P_k}{\partial t}+v_k g\cos\phi \tag{B-23}$$

Specific enthalpy can be written as a function of temperature and pressure,

$$\frac{\partial h_k}{\partial t}=Cp_k\frac{\partial T_k}{\partial t}-\eta_k Cp_k\frac{\partial P_k}{\partial t} \tag{B-24}$$

$$\frac{\partial h_k}{\partial z}=Cp_k\frac{\partial T_k}{\partial z}-\eta_k Cp_k\frac{\partial P_k}{\partial z} \tag{B-25}$$

where η_k is Joule–Thomson coefficient defined as:

$$\eta_k=0,\quad k=g \tag{B-26}$$

$$\eta_k=-\frac{1}{Cp_k\rho_k},\quad k=o,w \tag{B-27}$$

For the gas phase, substituting Eqs. (B-24), (B-25) and (B-26) into the Eq. (B-23), the gas energy equation is:

$$Cp_g\left[\frac{\partial T_g}{\partial t}+v_g\frac{\partial T_g}{\partial z}\right]+v_g\left[\frac{\partial v_g}{\partial t}+v_g\frac{\partial v_g}{\partial z}\right]-\frac{1}{\rho_g}\frac{\partial P}{\partial t}=-v_g g\cos\phi \tag{B-28}$$

For the oil and water phases, substituting Eqs. (B-24), (B-25) and (B-27) into the Eq. (B-23), the oil and water energy equations are:

$$\varepsilon_o\rho_o Cp_o\left[\frac{\partial T_o}{\partial t}+v_o\frac{\partial T_o}{\partial z}\right]+\varepsilon_o\rho_o v_o\left[\frac{\partial v_o}{\partial t}+v_o\frac{\partial v_o}{\partial z}\right]+\varepsilon_o v_o\frac{\partial P}{\partial z}=-\varepsilon_o\rho_o v_o g\cos\phi \tag{B-29}$$

$$\varepsilon_w\rho_w Cp_w\left[\frac{\partial T_w}{\partial t}+v_w\frac{\partial T_w}{\partial z}\right]+\varepsilon_w\rho_w v_w\left[\frac{\partial v_w}{\partial t}+v_w\frac{\partial v_w}{\partial z}\right]+\varepsilon_w v_w\frac{\partial P}{\partial z}=-\varepsilon_w\rho_w v_w g\cos\phi \tag{B-30}$$

The model was formulated for a flow without phase change and without heat transfer between it and its surroundings. Then one expects that the phases (oil, water and air) have constant temperatures. In fact this occurs for the oil and water, however, due to the gas compressibility, its temperature can change. Then with the idea of to take into account this phenomenon, the model was formulated as a thermal model.

In a thermal model the density is a function of temperature and pressure, but when the change of pressure or the compressibility is small, the flow can be considered as incompressible, and then oil and water have constant density. Under this condition the density is independent of the pressure and it represents the hydrodynamic pressure instead of the thermodynamic pressure.

On the other hand, the gas is a compressible phase then its pressure is a thermodynamic pressure, so an equation of state was used to describe the relation among pressure, temperature and density for the gas. However, it was supposed that there was no interfacial gradient pressure and that the bubbles were perfectly spherical, then the pressures of the three-phases were considered equals, but with different temperatures.

References

Bannwart, A., Vieira, F.F., Carvalho, C.H.M., Oliveira, A.P., 2005. Water-assisted flow of heavy oil and gas in a vertical pipe. In: SPE/PS-CIM/CHOA 97875. International Thermal Operations and Heavy Oil Symposium, Calgary, Alberta, Canada, 1–3 November.

Bonizzi, M., Issa, R.I., 2003. On the simulation of three-phase slug flow in nearly horizontal pipes using the multi-fluid model. Int. J. Multiphase Flow 29, 1719–1747.

Cazarez-Candia, O., Montoya, D., Vital, G., 2009. Mathematical model for bubbly water–heavy oil–gas flow in vertical pipes. J. Petrol. Sci. Technol. 27, 1715–1726.

Cazarez, O., Vazquez, M., 2005. Prediction of pressure, temperature and velocity distribution of two-phase flow in oil wells. J. Petrol. Sci. Eng. 46, 195–208.

Chung, M., Lee, S., 2001. Effect of interfacial pressure jump and virtual mass terms on sound wave propagation in the two-phase flow. J. Sound Vib. 244 (4), 717–728.

Clift, R., Grace, J.R., Weber, M.E., 1978. Bubbles, Drops and Particles. Academic Press, New York.

Dongarra, J.J., Bunch, J.R., Moler, C.B., Stewart, G.W., 1990. LINPACK user guide. Soc. Ind. Appl. Math., Philadelphia, Eighth printing.

Drew, D., Cheng, L., Lahey Jr., R.T., 1979. The analysis of virtual mass effects in two-phase flow. Int. J. Multiphase Flow 5, 233–242.

Espinosa-Paredes, G., Soria, A., 1998. Method of finite difference solution to the transient bubbly air–water flows. Int. J. Numer. Methods Fluids 26, 1155–1180.

Ghorai, S., Suri, V., Nigam, K.D.P., 2005. Numerical modeling of three-phase stratified flow in pipes. Chem. Eng. Sci. 60, 6637–6648.

Hatta, N., Fujimoto, H., Isobe, M., Kang, J.S., 1998. Theoretical analysis of flow characteristics of multiphase mixtures in a vertical pipe. Int. J. Multiphase Flow 24 (4), 539–561.

Hirsch, C., 1988. Numerical Computation of Internal and External Flows. John Wiley & Sons, New York.

Khor, S.H., Mendes-Tatsis, M.A., Hewitt, G.F., 1997. One-dimensional modeling of phase holdups in three-phase stratified flow. Int. J. Multiphase Flow 23 (5), 885–897.

Lahey, R., Cheng, L., Drew, D., Flaherty, J., 1980. The effect of virtual mass on the numerical stability of accelerating two phase flow. Int. J. Multiphase Flow 6, 281–294.

Lahey Jr., R.T., Drew, D.A., 1989. The three-dimensional time and volume averaged conservation equations of two-phase flow. Adv. Nucl. Sci. Technol. 20 (1), 1–69.

Lahey, R.T., 1992. Boiling Heat Transfer, Modern Developments and Advances. Elsevier, The Netherlands. pp. 31–83.

Linè, A., Leon-Becerril, E., 2001. Stability analysis of a bubble column. Chem. Eng. Sci. 56, 6135–6141.
Michele, V., Hempel, D., 2002. Liquid flow and phase holdup-measurement and CFD modeling for two and three phase bubble columns. Chem. Eng. Sci. 57, 1899–1908.
Mitra-Majumdar, D., Farouk, B., Shah, Y., 1997. Hydrodynamic modeling of three-phase flows through a vertical column. Chem. Eng. Sci. 52, 4485–4497.
Mitra-Majumdar, D., Farouk, B., Shah, Y., Macken, N., 1998. Two and three-phase flows in bubble columns: numerical predictions and measurements. Ind. Eng. Chem. Res. 37, 2284–2292.
Nikitopoulos, D.E., Michaelides, E.E., 1995. Phenomenological model for dispersed bubbly flow in pipes. AIChE J. 41 (1), 12–22.
No, H.C., Kasimi, M.S., 1985. Effects of virtual mass on the mathematical characteristic and numerical stability of the two fluid model. Nucl. Sci. Eng. 89, 197–206.
Oddie, G., Shi, H., Durlofky, L.J., Aziz, K., 2003. Experimental study of two and three phase flows in large diameter inclined pipes. Int. J. Multiphase Flow 29, 527–558.
Padial, N., VanderHeyden, W., Rauenzahn, R., Yarbro, S., 2000. Three dimensional simulation of a three-phase draft-tube bubble column. Chem. Eng. Sci. 55, 3261–3273.
Pauchon, C., Banerjee, S., 1986. Interphase momentum interaction effects in the averaged multifield model. Part I: void propagation in bubbly flows. Int. J. Multiphase Flow 12 (4), 559–573.
Park, J.W., Drew, D.A., Lahey, R.T., 1998. The analysis of void wave propagation in adiabatic monodispersed bubby two-phase flows using an ensemble-averaged two-fluid model. Int. J. Multiphase Flow 24, 1205–1244.
Ransam, V., et al., 1981. RELAP 5/MOD I, Code Manual. System Models and Numerical Methods. NUREG/CR-1826, vol. 1.
Ruggles, A., Lahey, R.T., 1988. An analysis of void propagation in bubbly flows. In: Proceedings of the 15th Miami International Symposium on Multiphase Transport and Particulate Phenomena.
Schallenberg, J., EnB, J., Hempel, D., 2005. The important role of local dispersed phase hold-ups for the calculation of three-phase bubble columns. Chem. Eng. Sci. 60, 6027–6033.
Shi, H., Holmes, J.A., Diaz, L.R., Durlofsky, L.J., Aziz, K., 2004. Drift-flux Parameters for Three-phase Steady-State Flow in Wellbores. SPE 89836, pp. 1–10.
Spedding, P.L., Woods, G.S., Raghunathan, R., Watterson, J., 2000. Flow pattern, holdup and pressure drop in vertical and near vertical two and three phase up flow. Chem. Eng. Res. Des. 78, 404–418.
Taitel, Y., Barnea, D., Brill, J.P., 1995. Stratified three phase flow in pipes. Int. J. Multiphase Flow 21 (1), 53–60.
Vieira, F., 2004. Escoamento trifásico vertical de óleos pesados aplicado à elevação artificial. Dissertação de mestrado. Thesis. Universidad de Campinas, Brazil.
Wang, F., Mao, Z., Wang, Y., Yang, C., 2006. Measurement of phase hold-ups in liquid–liquid–solid three-phase stirred tanks and CFD simulation. Chem. Eng. Sci. 61, 7535–7550.
Woods, G.S., Spedding, P.l., Watterson, J.K., Raghunathan, R.S., 1998. Three-phase oil–water–air vertical flow. Trans. ICheE 76, 571–584.
Zhang, H.Q., Sarica, C., 2005. Unified Modeling of Gas/Oil/Water Pipe Flow-basic Approaches and Preliminary Validation. SPE 95749, pp. 1–9.